

# The impact of resolution and formulation on model simulations of an east coast low

B.W. Golding\* and L.M. Leslie

Bureau of Meteorology Research Centre, Australia

(Manuscript received September 1992; revised February 1993)

Australian east coast lows are severe weather events that involve synoptic and sub-synoptic-scale processes. As such, it is of interest to examine the sensitivity of numerical simulations both to model formulation, and to model resolution.

In this study, two models were used: a version of the current operational regional model (RASP) of the Australian Bureau of Meteorology that contains an improved representation of the boundary-layer processes; and the non-hydrostatic mesoscale model of the UK Meteorological Office (UKMO) which was designed specifically for very high resolution prediction.

The RASP model was run at three different horizontal resolutions: 150 km (the current operational resolution), 50 km and 15 km. The UKMO model was run only at 15 km, which is within its design range.

The east coast low of 31 July–2 August 1990 was chosen for the sensitivity study. Large gains in accuracy were obtained in the RASP model simulations as the resolution was increased. This was true of all key variables including mean sea level pressure, low-level wind field strength and structure, and rainfall amounts and distribution. However, the RASP model simulations at 15 km were beginning to show some signs that the convection scheme was not appropriate for such high resolutions. The UKMO model simulation was generally of similar quality to the RASP model forecasts, but was slightly superior in the depiction of rain-band shape and coastal wind values.

In summary, it is clear from the simulations that increasing the resolution of RASP leads to improved forecasts of Australian east coast lows. However, an equally important finding is that the improvement cannot go on indefinitely as at very high resolutions the representation of some physical processes in the model should be designed specifically for use at these high resolutions.

## Introduction

A major weather-related cause of damage in Australia is flooding. Storms of many kinds contribute to this problem, including severe convective storms, tropical cyclones and synoptic-scale depressions. Of particular importance to the east coast is a class of depressions known as east coast lows. Holland et al. (1987) identified three types of east coast low, of which the second was by far the most common, producing one or more major flooding events per year. Their analysis found that these systems are most common in late winter and

early spring, and develop within a slow-moving trough in the subtropical easterly flow near eastern Australia, which is known there as an 'easterly dip'. A mid-tropospheric cut-off cold pool normally lies to the west of the developing trough. The east coast low develops within the trough and moves southwards along the coast. At the same time, anticyclonic development occurs to the south resulting in a strengthened easterly gradient. Where this impinges on the Great Dividing Range of southeastern Australia, heavy rainfall occurs. Within the synoptic-scale low, a subsidiary warm core centre with hurricane-force winds may be observed.

The aims of this study are two in number. The first is to examine the performance of a research

\*Permanent affiliation: United Kingdom Meteorological Office.

Corresponding author address: Dr L.M. Leslie, Bureau of Meteorology Research Centre, GPO Box 1289K, Melbourne, Vic 3001, Australia.

version of the current operational RASP as the horizontal resolution of the model is improved. The research version contains an enhanced representation of physical processes, particularly of the boundary-layer turbulent transports. Model simulations with the research RASP are carried out at the current operational horizontal resolution of 150 km, and also at 50 km and 15 km. The second aim is to compare the RASP simulations with those of the UKMO mesoscale model which was designed specifically to operate at very high resolutions, and also is non-hydrostatic. Here, the interest centres on the impact of model formulation, especially in relation to assessing how appropriate the RASP model is at very high resolutions (20 km or less) and for complex systems like east coast lows where moist physical processes play a crucial role.

Previous numerical studies (Leslie et al. 1987; Hess 1990; McInnes and Hess 1992), using versions of the Australian Bureau of Meteorology's regional forecasting system (RASP), have shown that development of the synoptic-scale system can be well predicted, and that rainfall accumulations increase towards the observed values as the resolution is refined. In the present study, simulations of one such storm using the RASP model are compared with a 15 km resolution simulation using a version of the United Kingdom Meteorological Office (UKMO) mesoscale model. Analysis of the results concentrates on assessing three aspects: the accuracy of the UKMO simulation; the benefits of using a purpose-built model for such high resolutions; and the benefits of fine resolution (15 km) relative to that currently used operationally (150 km). The models are described in the next section. Then follows a description of the event used for the study. The model results are presented and discussed in the final two sections.

## Model descriptions

### The Bureau of Meteorology regional forecasting system (RASP)

RASP has been used in several previous studies of east coast lows. Here we use the form described in McInnes and Hess (1992). The adiabatic formulation, described in Leslie et al. (1985), is hydrostatic with a terrain-following ( $\sigma$ ) vertical coordinate, and uses a semi-implicit time integration. In the present experiment, fourteen levels are used at  $\sigma$  values of: 0.999, 0.99, 0.98, 0.95, 0.9, 0.85, 0.8, 0.7, 0.6, 0.5, 0.4, 0.3, 0.2, 0.1. Surface exchanges are computed using Monin-Obukhov similarity theory, with a three-layer soil model (Louis 1984) defining the moisture availability at the surface. The surface temperature is computed using a surface heat budget in which the radiation is computed using Paltridge and Platt (1976 ch. 6)

and the soil heat flux is obtained from a three-level soil model similar to Louis (1984). A level 2.25 turbulent diffusion scheme based on Galperin et al. (1988) is used for boundary-layer diffusion. This scheme predicts turbulence as a function of shear, buoyancy and dissipation, but makes no allowance for subgrid-scale condensation and evaporation. The mixing length is diagnosed from the turbulence profile. Precipitation in the model can be either stable or convective, but not both at the same grid-point (Hess 1990). The distinction depends on the conditional stability of the grid column. Stable precipitation occurs when the humidity exceeds 90 per cent for all model runs, and condensate falls directly to the ground with allowance for evaporation following Kessler (1969). The deep convection scheme is based on Hammarstrand's (1977) modification of the Kuo (1965) scheme.

In the experiments described here, RASP was first run on its operational domain with a resolution of 150 km for 48 hours from an initialisation valid at 2300 UTC 30 July 1990. During the first 24 hours, predicted fields were nudged towards 12-hourly analyses, which is a standard data assimilation procedure for reducing 'spin-up' at the beginning of a model forecast. The results for the second 24 hours are described later. They also provide the initial and boundary conditions for the finer resolution experiments with both models. In these experiments, RASP was run on a  $52 \times 52$  grid on a Lambert Conformal projection with resolutions of 50 km and 15 km, the latter being the finest that could be accommodated. In both runs, initial conditions were adjusted to fine-scale orography derived from the NCAR  $5' \times 5'$  latitude - longitude data set. The sea-surface temperatures were obtained by interpolation from a 150 km resolution monthly climatology.

### The UKMO mesoscale model

The second model used in this study is the latest version of the United Kingdom Meteorological Office (UKMO) mesoscale model. This is a fully compressible, non-hydrostatic atmospheric model with parametrisations of subgrid-scale processes developed specifically for mesoscale resolution. It uses height as the vertical coordinate. The model's adiabatic formulation is described in Golding (1992a). In order to overcome the timestep restrictions imposed by an equation set that supports sound waves, a semi-implicit time integration is used in which the linearised sound and gravity wave equations are treated implicitly with an explicit forcing from the non-linear terms. To further improve stability with long timesteps, advection is treated using a third order semi-Lagrangian scheme (Staniforth and Côté 1991).

Turbulent diffusion is parametrised using a level 2.5 scheme as described in Ballard et al.

(1991). This scheme predicts turbulent kinetic energy as a function of shear, buoyancy and dissipation. The buoyancy terms allow for subgrid-scale condensation and evaporation. A by-product of the scheme is specification of the mean and variance of the subgrid-scale relative humidity, from which an estimate of cloud fraction is obtained. Rain and ice are generated by microphysical interactions within the cloud and are then advected separately. The parametrisation is derived from Cox (1988) but with ice cloud, snow and graupel combined. The faster acting microphysical processes are treated implicitly and a special treatment of the vertical fluxes permits timesteps longer than the time of fall through each layer.

A five-band long wave radiation scheme (Roach and Slingo 1979) and a single-band short wave scheme (Somieski 1988) are used, with modification to incorporate the detailed cloud fraction and density information generated in the turbulence and microphysical parametrisations. A two-layer soil scheme is coupled to the surface heat budget and atmospheric fluxes are obtained from pre-computed Monin-Obukhov transfer functions as a function of Richardson Number and roughness length. Charnock's formula (Charnock 1955; Wu 1982) is used for roughness over the sea. Over land, roughness is specified taking account of subgrid-scale orography:

$$Z_0 = \text{MIN} (0.3 + 0.0001 E, 1.0) \text{ metres,}$$

where  $E$  is the land height. The roughness length for heat is

$$Z_T = 0.00025/Z_0 \text{ metres.}$$

A fuller and more correct way of writing this equation is:

$$Z_T = Z_{TL}/(Z_0/Z_{0L})$$

where  $Z_{0L}$ ,  $Z_{TL}$  are the local momentum and heat roughness lengths, respectively, of the dominant vegetation, and  $Z_0$ ,  $Z_T$ , are the heterogeneous roughness lengths accounting for local orography, trees, buildings, etc. For use in the model, it has been assumed here that  $Z_{0L} = 0.05\text{m}$ , uniform over the full domain;  $Z_{TL} = 0.005\text{m}$ , uniform over the full domain; and  $Z_0$  varies linearly with orographic height. The albedo is set to 0.2 over land. Moisture transfer is controlled by a resistance to evaporation (Monteith 1964) which is overridden at night or when rain has accumulated on the surface. A constant value of  $100 \text{ s m}^{-1}$  is used in the model for the surface resistance.

Subgrid-scale convection is parametrised using the scheme described in Golding (1992b), based on Fritsch and Chappell (1980). This differs from other parametrisations in its handling of the mass redistribution. Instead of computing the compensation subsidence, mass fluxes resulting from the up and downdraught calculations are provided as

forcing terms to the non-hydrostatic continuity equation, allowing the model dynamics to determine the scale of the response as a function of the background state and the distribution of convective clouds.

In the simulation presented here, the model was run with a 15 km resolution over a  $90 \times 100$  domain on a local transverse Mercator projection. A one-minute timestep was used, but similar results were obtained with a three-minute timestep. Initial and boundary conditions from the coarse RASP simulation are reprojected and interpolated to height levels relative to the fine orography. Sea-surface temperatures were interpolated from the same 150 km resolution climatology as was used for RASP.

## Case description

The case chosen for study in this paper was the first of two east coast lows that affected the east coast of Australia in the period 30 July to 3 August 1990. Although not as strong a vortex as the second, the intensity of the easterly flow between the low and the anticyclone to the south produced exceptionally large rainfall accumulations over the coast and mountains to the south of Sydney, reaching 200 mm in 24 hours in some locations. An easterly dip was first evident in the surface pressure field on 29 July (Fig. 1(a)). During the period 30–31 July, a surface centre formed and moved south (Fig. 1(b),(c)). It was mirrored by sharpening of a mid-tropospheric trough into a cut-off vortex to the west (not shown). At the same time, an anticyclone moved eastwards to the south of the continent, increasing pressure gradients on the south side of the low. During 1 August (Fig. 1(d)), the low moved close into the coast, with only a small fall in central pressure, and finally crossed the coast, dissipating inland during 2 August. The model intercomparison concentrates on the 24-hour period from 2300 UTC 31 July to 2300 UTC 1 August during which the easterly gradient on the south side of the system was at its maximum, producing the largest rainfall rates. Figure 2 shows the BMRC hand-drawn analysis for 1100 UTC 1 August. At 500 hPa (Fig. 2(a)) a large cut-off low lies over the east of the continent. At the surface, (Fig. 2(b)) pressure gradients are strong to the south of the low, where high pressure is maintained in the anticyclone, and along the coast. There are few observations out to sea, but where they exist, they indicate a trough extending eastwards from the centre with very strong winds to the south.

The satellite image (Fig. 3) shows deep convective cloud over the coast near the centre, and bands of high cloud possibly from deep slantwise ascent over the baroclinic gradient associated with the trough. A second bright spot associated

**Fig. 1** Operational mean sea level pressure analyses for (a) 2300 UTC 29 July, (b) 2300 UTC 30 July, (c) 2300 UTC 31 July, (d) 2300 UTC 1 August 1990. Contour interval 4 hPa.

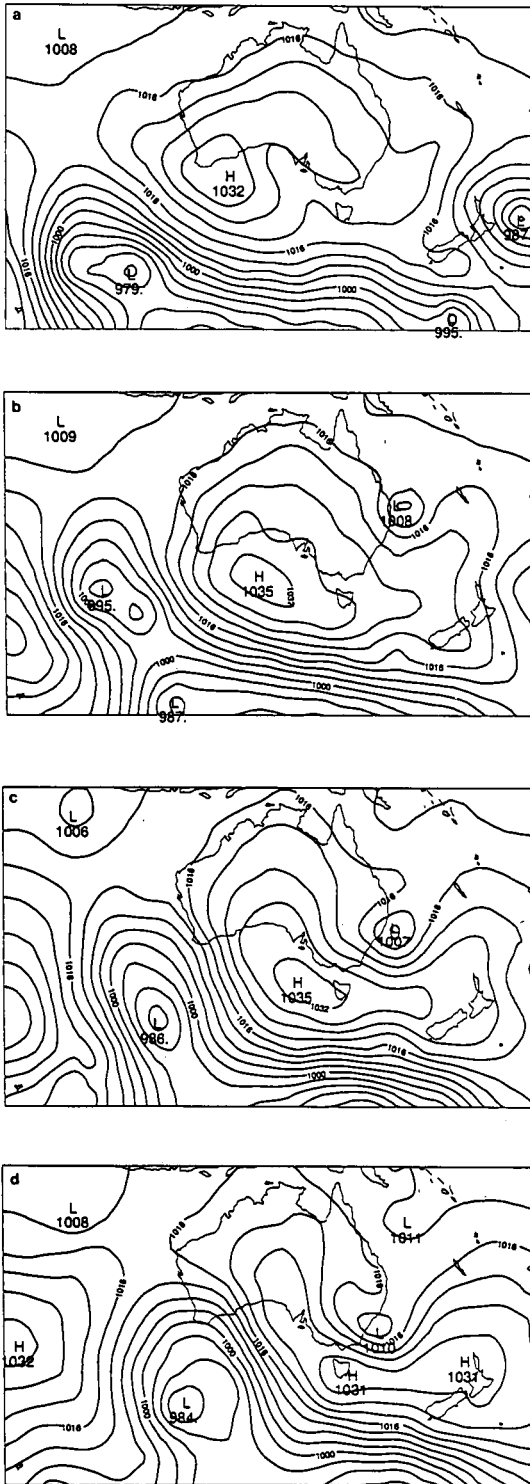
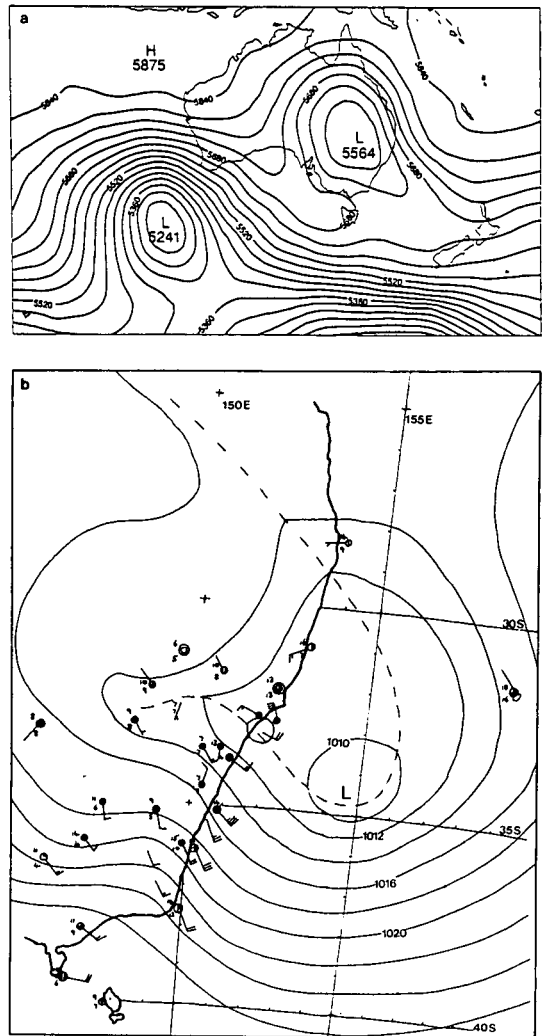


**Fig. 2** Analyses for 1100 UTC 1 August 1990: (a) 500 hPa heights — interval 60 gpm; (b) surface observations and pressure analysis (contours in hPa).



with upright convection is identifiable to the southeast of the centre. Experience shows that in the north Atlantic, similar poleward-moving depressions are sometimes observed on the eastern side of a stationary upper tropospheric trough. The analysis used in the UK for such systems places a warm occlusion in the east-west trough. A triple point is analysed to the east where the cyclonic side of the upper jet exit reinforces the low-level baroclinic development. The structure of the present system seems to be similar. Although structures of these fronts are very different from the progressive Norwegian model, a trajectory analysis of a numerical simulation of one such case (Golding 1981, 1986) showed that

Fig. 3 **GMS infrared satellite images for southeast Australia 1 August 1990: (a) 0830 UTC; (b) 1130 UTC; (c) 1430 UTC.**

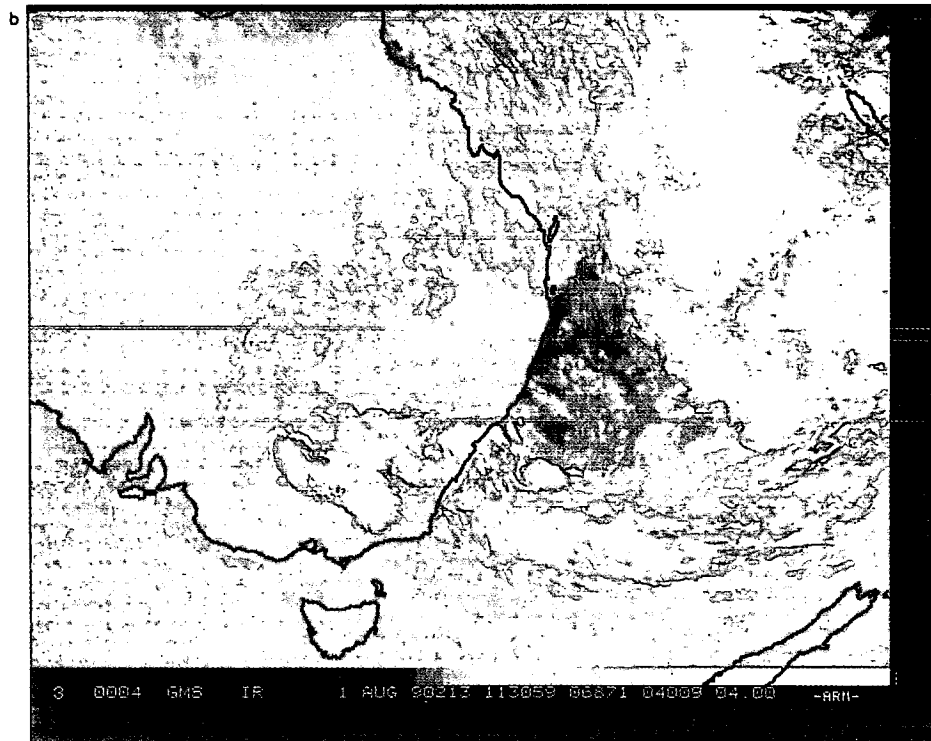
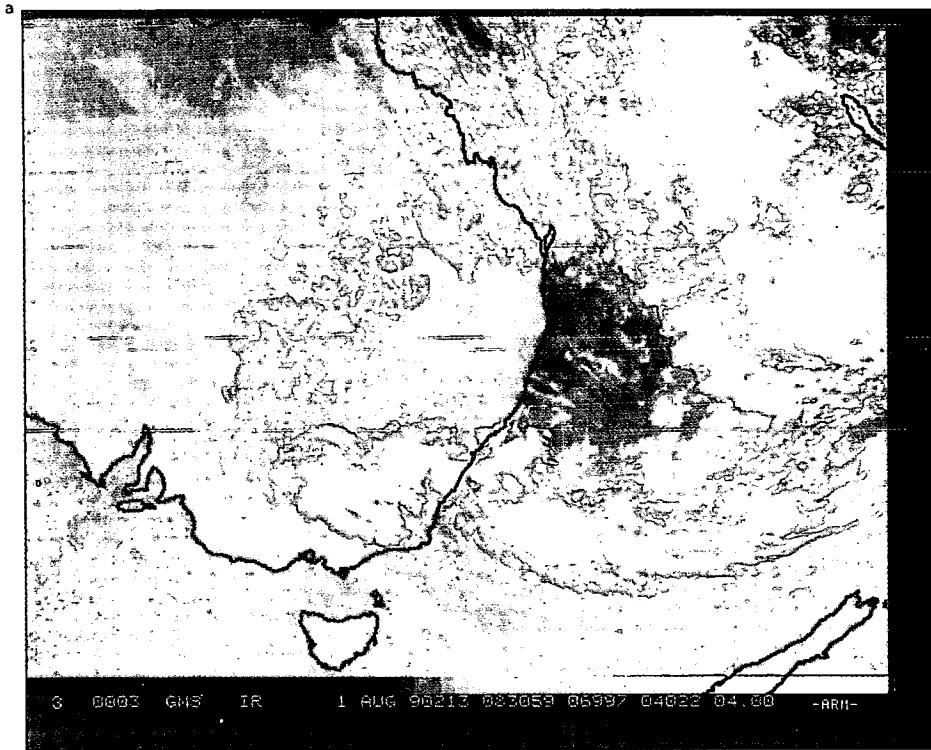
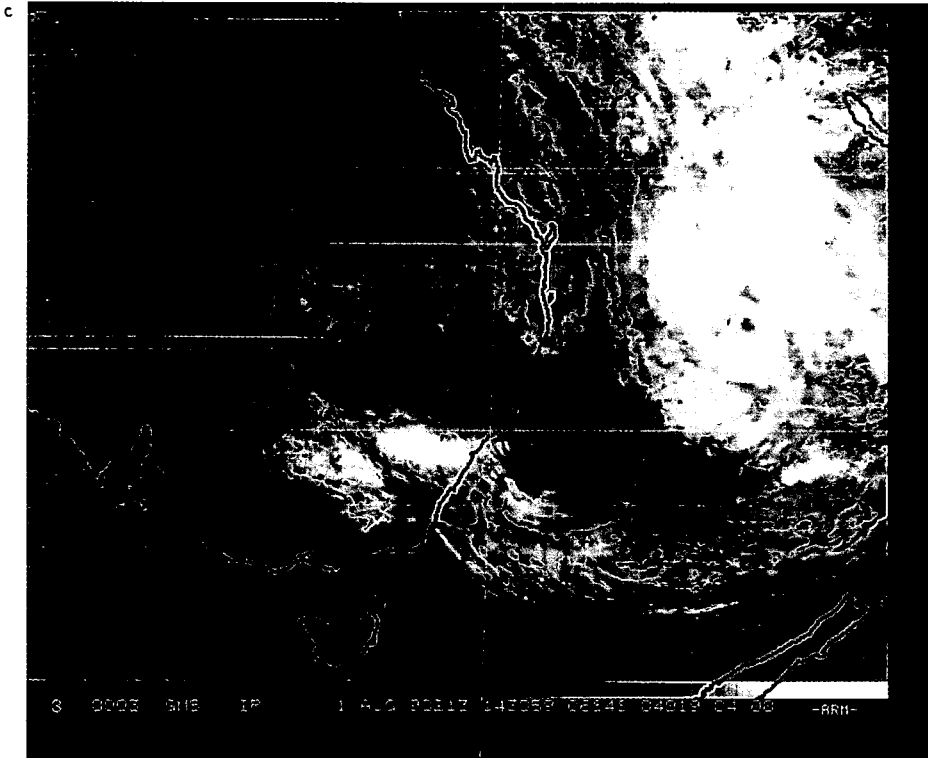


Fig. 3 Continued.



the kinematic structure is similar. This analysis indicated that surface air parcels moving poleward relative to the system, turned west (east) as they ascended the frontal surface if they rose to the west (east) of this triple point.

As described above, this case shows the characteristics of the type two east coast lows discussed in Holland et al. (1987). In particular, the subsidiary development of a small vortex close to the coast is evident in the 1100 UTC 1 August analysis. The 24-hour rainfall for the period up to 2300 UTC 1 August is shown in Fig. 4, but it should be noted that substantial falls also occurred the previous day, and continued until the clearance of the second system on 3 August. Falls of over 100 mm were confined to coast facing slopes of the Great Dividing Range from Newcastle in the north to Jervis Bay in the south, extending inland to near Bathurst. The time history of rainfall at Robertson, where the highest recorded total fell, is shown in Fig. 5. The peak sustained rain rate is about  $45 \text{ mm h}^{-1}$  between 0700 and 0715 UTC.

Fig. 4 24-hour rainfall totals ending at 2300 UTC 1 August 1990.

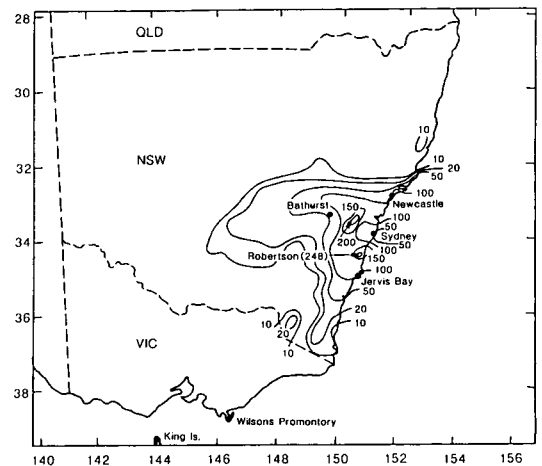


Fig. 5 Hourly rainfall totals extracted from Robertson pluviograph for 1 August 1990.

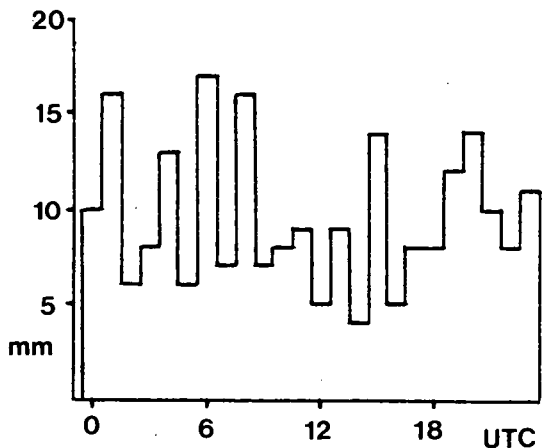
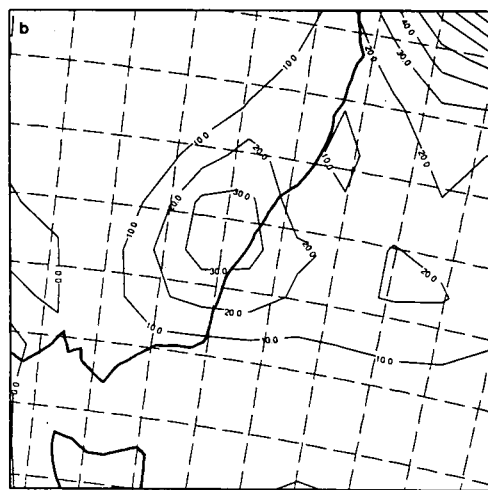
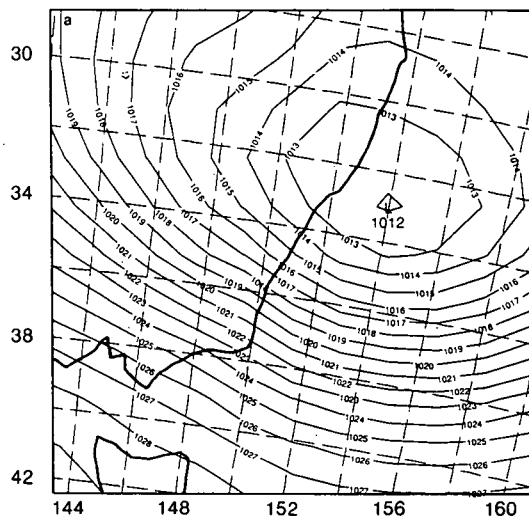


Fig. 6 150 km mesh RASP results. (a) Mean sea level pressure at 1100 UTC 1 August 1990 — contour interval 1 hPa. (b) Rainfall total for 24 hours ending 2300 UTC 1 August 1990 — contour interval 10 mm.



### Model simulations

In this section, the model simulations will be described, proceeding from the coarsest to finer resolutions. The analysis will concentrate on surface characteristics at 1100 UTC 1 August 1990, together with the 24-hour rainfall accumulation for the period to 2300 UTC 1 August.

#### 150 km RASP

This simulation produced a rather symmetric low with a good position and central pressure (Fig. 6(a)). There is no indication of orographic distortion of the pressure field, and only a slight enhancement of the 850 hPa wind over the mountains (not shown). The low moves inland by 2300 UTC as observed. Although the gradient to the south of the centre intensifies a little, the strongest surface winds at 1100 UTC are  $15 \text{ m s}^{-1}$  over the sea at  $37^\circ\text{S}$ , although slightly higher values are present earlier in the integration. The 24-hour precipitation accumulation (Fig. 6(b)) reaches 20 mm over the sea and 30–40 mm over high ground. About one-third of this is stratiform and the rest convective. The performance of the RASP model at this resolution was typical of the predictive skill of east coast lows in operational prognoses by the National Meteorological Centre.

#### 50 km RASP

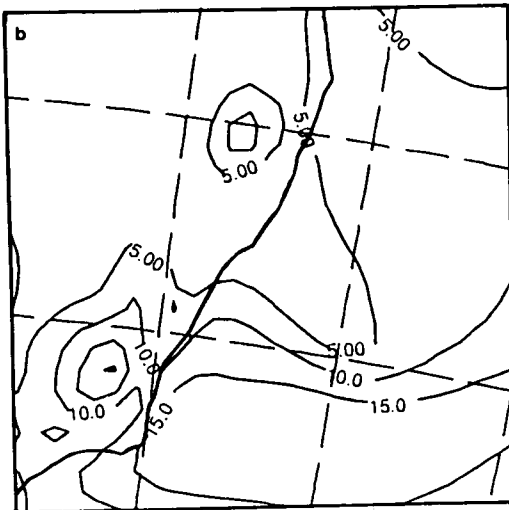
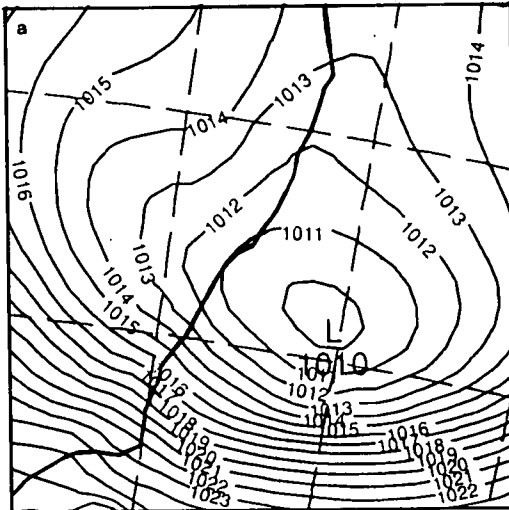
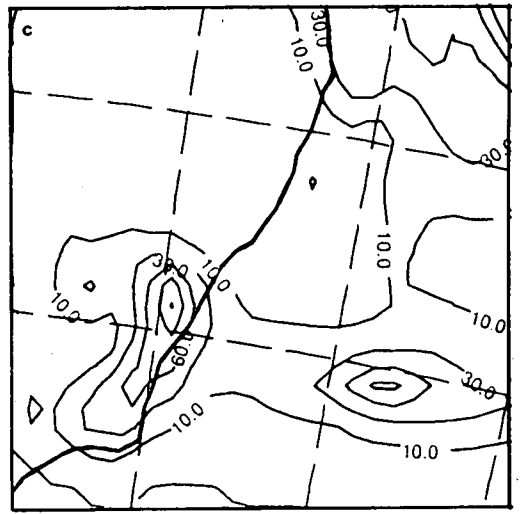
This simulation produces a deeper low with a strong gradient to the south and a more marked east-west trough (Fig. 7(a)). A single centre is maintained which again moves inland by 2300 UTC. There is little evidence of orographic pressure effects, but the 850 hPa wind is enhanced to

more than  $20 \text{ m s}^{-1}$  over the mountains (not shown). The surface wind (Fig. 7(b)) reaches a maximum of  $15\text{--}20 \text{ m s}^{-1}$  over the sea at  $36\text{--}38^\circ\text{S}$ , and also over the mountains. The 24-hour precipitation (Fig. 7(c)) is enhanced about fourfold, with maxima of 90 mm over the sea, and 120 mm over the mountains. However the totals are too low by a factor of at least two. Over half of the precipitation is convective. A result of the enhanced convective activity is a slight excess in the upper-level cloud amount. Overall, the quality of the RASP simulation at this resolution is markedly superior to the prediction at 150 km.

**15 km RASP**

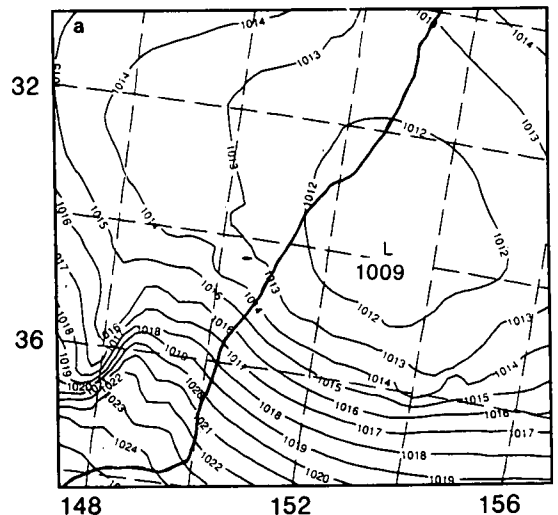
This simulation shows much more detail in the pressure field (Fig. 8(a)) with the centre moving close into the coast well before the system moves over land. There is also a deep trough in the lee of the mountains and some perturbations over the sea in regions of strong diabatic forcing. The low deepens a little further in this simulation, to 1009 hPa, and there is less evidence of the east-west trough. The surface wind has a broad region of 15–20 m s<sup>-1</sup> from 35.5–38.5°S and develops a local maximum southeasterly of over 20 m s<sup>-1</sup> as

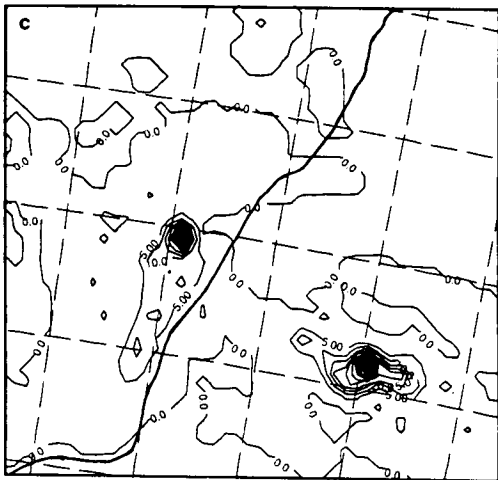
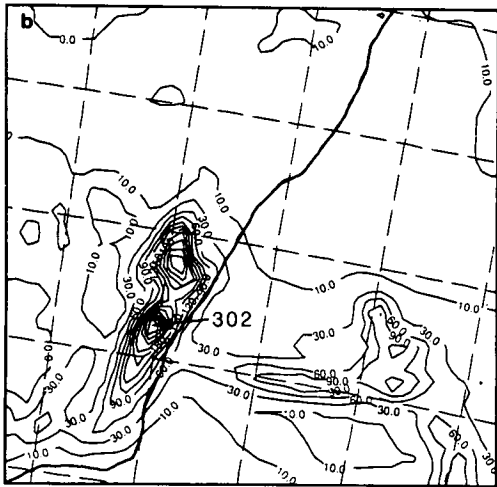
**Fig. 7** 50 km mesh RASP results. (a) Mean sea level pressure at 1100 UTC 1 August 1990 — contour interval 1 hPa. (b) 1000 hPa wind speed at 1100 UTC 1 August 1990 — contour interval 5 m s<sup>-1</sup>. (c) Rainfall total for 24 hours ending 2300 UTC 1 August 1990 — contours at 0, 10, 30, 60, 90, 120 mm.



the low makes landfall at 1800 UTC. There is considerable enhancement of the 850 hPa wind over the mountains (not shown). The 24-hour rainfall (Fig. 8(b)) is approximately doubled, with a maximum of 150 mm at sea and a maximum of just above 300 mm over the mountains, which is possibly a little too high. Rather more than half of this is convective precipitation. The large falls are restricted to the coast facing slopes. There is a deterioration in the representation of cumulus convection in the model in that an examination of the rain rate (Fig. 8(c)) shows excessive rates

**Fig. 8** 15 km mesh RASP results. (a) Mean sea level pressure at 1100 UTC 1 August 1990 — contour interval 1 hPa. (b) Rainfall total for 24 hours ending 2300 UTC 1 August 1990 — contours at 0, 10, 30, 60, ... 360 mm. (c) Rainfall rate at 1100 UTC 1 August 1990 — contour interval 5 mm h<sup>-1</sup>.





from the convection scheme at several isolated grid-points. The mean sea level pressure field (Fig. 8(a)) is shown here without the usual application of a light filter prior to display, in an attempt to emphasise the small spurious effects in the vicinity of the precipitation rate maximum. The implication is that the cumulus parametrisation is becoming inappropriate for this resolution in its present form, as will be discussed later.

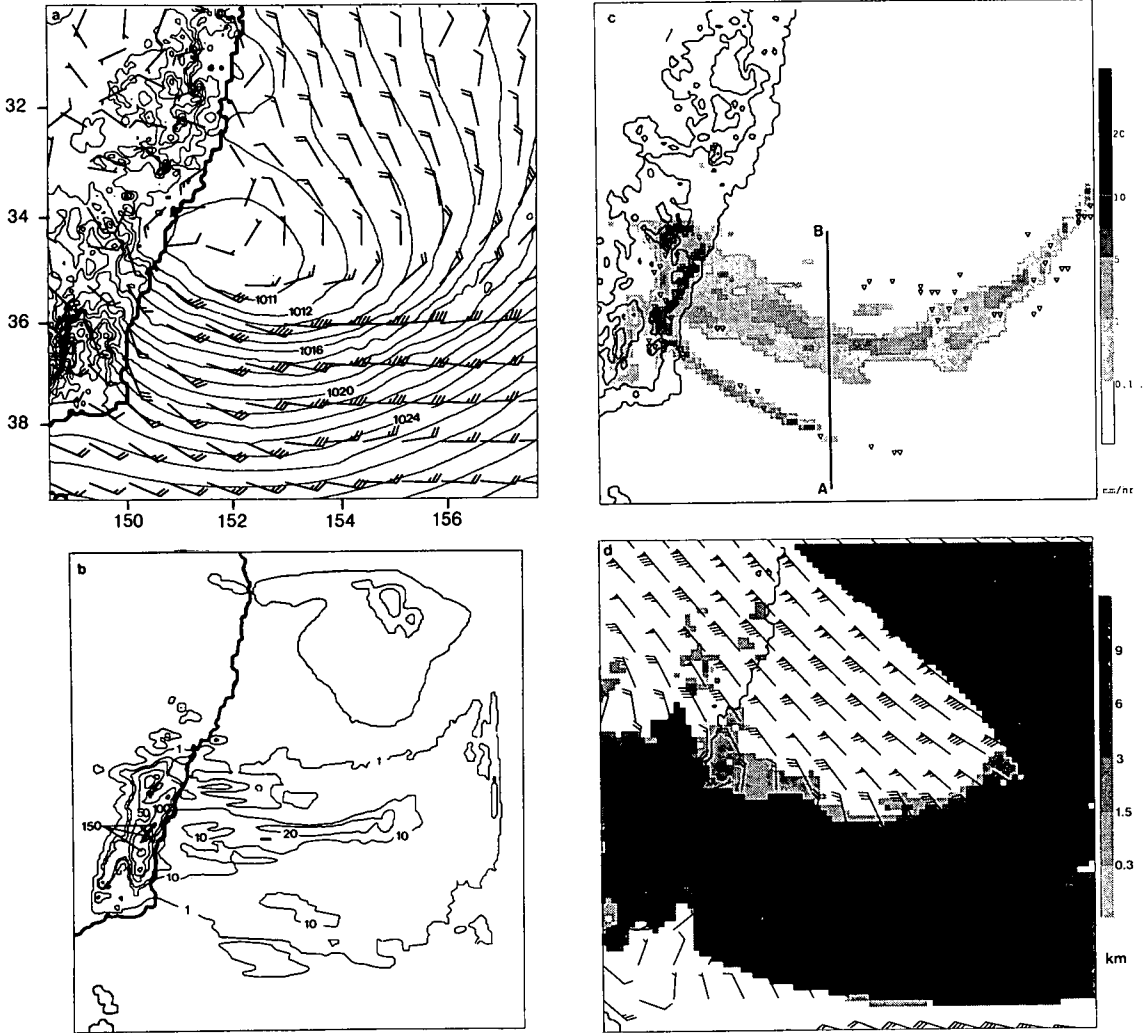
#### 15 km UKMO model

This simulation gives a good shape to the low (Fig. 9(a)), again without the observed subsidiary circulation to the north of Sydney. However, note the  $7.5 \text{ m s}^{-1}$  southwesterlies near the coast here. The position is good and the overall pressure is about 1 hPa too high. The location and strength of the coastal winds south of Sydney are well captured (see Fig. 2(b)). Note that the strongest winds, of  $25 \text{ m s}^{-1}$ , are associated with the main rain-band here and are somewhat further north than in the RASP results. Gradients to the east

and north are slack, in agreement with the observation at Lord Howe Island. The enhanced roughness over land produces accurate wind speeds there, most being  $10 \text{ m s}^{-1}$  or less. The rainfall accumulation (Fig. 9(b)) is too small around Newcastle and perhaps a little high further south where the maximum is 305 mm, which is remarkably close to that produced by the 15 km RASP. Note the isolated higher values over the sea near Newcastle, indicating convective activity, in agreement with Fig. 3(a) but less than the amounts observed, and over the sea rather than the coast. The extension of high accumulations to the west of Sydney matches well with the observations. The predicted rainfall comes predominantly from stratiform cloud processes, convection contributing only about 10 mm to the total over the mountains. The rainfall maximum over the sea in the northern part of the domain is spurious and arises from the boundary conditions. It affects only the latter part of the simulation. The rainfall rate prediction for 1100 UTC is shown in Fig. 9(c). A rather narrow band is evident, which broadens toward the coast. The detached rain-band to the south results from an isolated line of upward motion contrasting with the slantwise ascent of the main band. A similar feature is evident in Fig. 3(c) at 1400 UTC. Precipitation on the mountains is largely independent of the pattern out to sea, depending only on the onshore wind and the orographic gradient. The cloud-top structure (Fig. 9(d)) shows the large clear area to the north of the low which was evident in Fig. 3 but largely lost in the finer RASP runs (not shown). High cloud to the northeast and south also agrees well with the imagery. Figure 10 shows a time series of hourly rainfall accumulations at the location of highest 24-hour total (point 'X' in Fig 9(b)) for comparison with Fig. 5. It shows underprediction for the first few hours due to spin-up from the 150 km resolution initialisation, followed by several hours with values close to the observed, and then a general overprediction for the latter part of the forecast.

Details of the rain-band structure are shown in Fig. 11. The main rain-band is on the right, and shows gentle ascent at low levels, followed by rather steep ascent of about  $0.25 \text{ m s}^{-1}$  near the freezing level. Beneath this is a weak evaporatively driven downdraught and, to its left, a second maximum of low-level uplift, associated with the second rainfall maximum. The upper tropospheric circulation is characteristic of moist symmetric instability, with a relatively steep upward branch and a shallower downward branch to the south. The structure of the detached squall to the left is not clear, though it seems to be associated with the return flow from the main rain-band and with low-level evaporative cooling. Note that the vectors shown here do not constitute streamlines as the dominant flow is normal to the section.

**Fig. 9** 15 km mesh UKMO results. (a) Mean sea level pressure (contour interval 1 hPa) and 10 m wind (feathered arrows) at 1100 UTC 1990. (b) Rainfall total for 24 hours ending 2300 UTC 1 August 1990 — contours at 1, 10, 20, 50, 100, 150 mm. (c) Rainfall rate at 1100 UTC 1 August 1990: stratiform (stipple — see key); convective (triangles 0.4–2 mm h<sup>-1</sup>), orography contours superimposed (interval 500 m). (d) Cloud top at 1100 UTC 1 August 1990 (stipple — see key) and wind at 9110 m (feathered arrows). The feathered arrows have their usual meanings.



**Discussion**

**Accuracy of the RASP simulations**

The research version of the current operational RASP was run at horizontal resolutions of 150 km, 50 km and 15 km. The performance of the RASP model corroborates that of earlier work (Leslie et al. 1987; Hess 1990; McInnes and Hess 1992) by exhibiting large gains in accuracy of prediction of the major quantities of interest as the grid-length decreases. For example, the RASP simulation at the current operational resolution of 150 km depicted the low-level wind values and

patterns quite poorly (not shown), and grossly underpredicted the rainfall amount, while simultaneously failing to capture the structure of the rain-bands. This is not surprising considering the size of the rain-bands. At the higher resolutions, the RASP simulations were much better, with stronger winds and precipitation forecasts that were more realistic in amount and pattern. However, there were some signs, especially as seen in Fig. 8(c), that the parametrisation of cumulus convection in the model was becoming inappropriate at the very high resolution of 15 km.

Fig. 10 Hourly rainfall totals for 1 August 1990 at location X in Fig. 9(b).

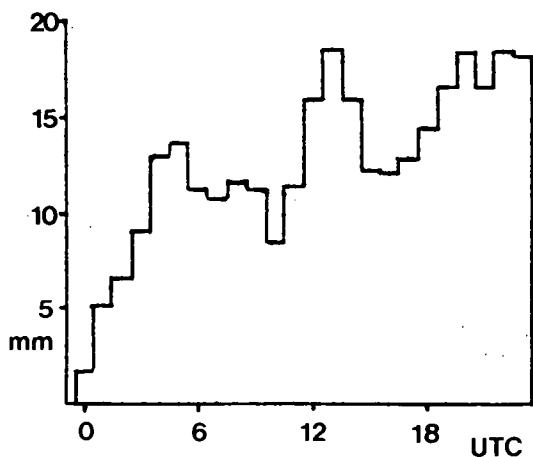
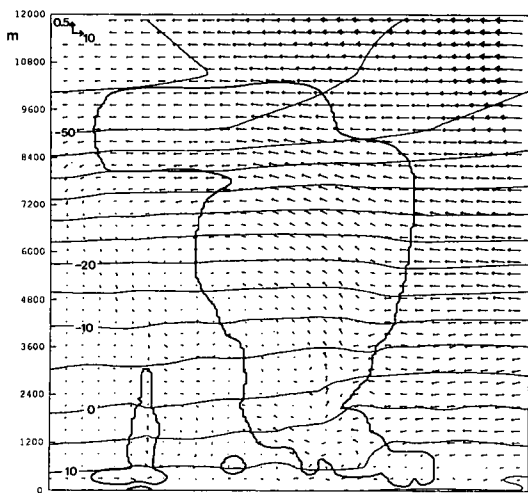


Fig. 11 Vertical section along A-B in Fig. 9(c) showing flow in the plane of the section (arrows in  $\text{m s}^{-1}$ , see scale in upper left-hand corner), temperature (light contours in  $^{\circ}\text{C}$ ) and cloud envelope.



#### Accuracy of the UKMO model simulation

The results presented in Fig. 9 generally agree well with the observations. Locations of the maximum rainfall accumulations are well depicted, and the rain-band structure looks realistic when compared with satellite imagery. Peak values of the 24-hour rainfall accumulation are rather higher than observed, but within observational error. Details of the time sequence of rain at Robertson cannot be matched against the model sequence, though the general level of the hourly totals is reproduced. The coastal winds are particularly good.

#### Benefits of a purpose built model

Comparison of the UKMO results with those from RASP at 15 km resolution indicates that the benefits of the former probably arise from better matching of the physical parametrisations to the resolution. There is no evidence that non-hydrostatic effects are important. However, the treatment of the lower boundary is superior, as indicated by the wind speeds over land, and there are some problems with the convection parametrisation in RASP when used at this resolution.

#### Benefits of fine resolution

Comparison of the RASP runs, bearing in mind the problems caused by tuning of the parametrisations as indicated above, confirms the benefits of finer resolution shown by earlier studies (Hess 1990). The influence of the orography on the pressure evolution is very evident and shows clear benefits of moving to the finest resolution in order to resolve as much orographic detail as possible. Over the sea, the winds are substantially improved at 50 km resolution relative to the winds at 150 km which were too weak (not shown). The rainfall accumulations also show substantial improvement, though are perhaps slightly too high at the finest resolution, probably due to the breaking down of the assumptions present in the Kuo cumulus convection parametrisation. Most notable of these assumptions is that a model volume contains an ensemble of cumulus elements. Clearly this is not the case on many occasions when the horizontal grid resolution drops to 15 km.

## Conclusions

Simulations of an east coast low event on 1 August 1990 were presented using two models and several grid resolutions. The models were a research version of the current operational Australian region system (RASP) and a version of the UK Meteorological Office's mesoscale model. The results of the simulations confirm the benefits of finer resolution found in earlier studies. Such benefits were noted in the pressure, wind and accumulated precipitation.

A significant finding of the study, through a comparison of the two models, is that further gains in accuracy arise when the physical parametrisations are tuned to the resolution. This was particularly evident in the low-level winds over land, and in the instantaneous rain rate.

Results from the UKMO simulation were compared in detail with observations and found to agree extremely well. These results are in accordance with results from earlier versions of the same model in the United Kingdom (Golding 1990). The RASP simulations were generally of similar quality to the UKMO model except that there

were some signs of deterioration, especially in the rainfall patterns, as the model resolution became too high for the assumptions present in the representation of some of the physical processes, most obviously the cumulus convection.

## Acknowledgments

The authors would like to express their appreciation to Mike Manton and John McBride of BMRC for stimulating discussions. We are indebted to Keith Colls and colleagues at the Sydney Regional Office of the Australian Bureau of Meteorology for providing the observational data. We are also grateful to David Pike of the Bureau of Meteorology Research Centre for assistance in preparing the diagrams.

## References

- Ballard, S.P., Golding, B.W. and Smith, R.N.B. 1991. Mesoscale model experimental forecasts of the Haar of North East Scotland. *Mon. Weath. Rev.*, *119*, 2107-23.
- Charnock, H. 1955. Wind stress on a water surface. *Q. Jl R. met. Soc.*, *81*, 693-40.
- Cox, G.P. 1988. Modelling precipitation in frontal rainbands. *Q. Jl R. met. Soc.*, *114*, 115-27.
- Fritsch, J.M. and Chappell, C.F. 1980. Numerical prediction of convectively driven pressure systems Part I: Convective parameterization. *J. Atmos. Sci.*, *37*, 1722-33.
- Galperin, B., Kantha, L. and Rosati, A. 1988. A quasi-equilibrium turbulent energy model for geophysical flows. *J. Atmos. Sci.*, *45*, 55-62.
- Golding, B.W. 1981. Diagnostic studies of mid-latitude depressions. Ph.D. thesis. University of Reading, England. (Copy available in National Meteorological Library, Bracknell, Berkshire RG12 2SZ, England.)
- Golding, B.W. 1986. A study of the structure of mid-latitude depressions in a numerical model using trajectory techniques. II: Case studies. *Met O 11 Technical Note No. 226*. (Unpublished, copy available in National Meteorological Library, Bracknell, Berkshire RG12 2SZ, England.)
- Golding, B.W. 1990. The Meteorological Office mesoscale model. *Met. Mag., Lond.* *119*, 81-96.
- Golding, B.W. 1992a. An efficient non-hydrostatic forecast model. *Met. Atmos. Phys.* (in press).
- Golding, B.W. 1992b. Numerical predictions of a severe storm in Melbourne. *Aust. Met. Mag.*, *42*, 47-57.
- Hammarstrand, U. 1977. On parameterization of convection for large scale numerical forecasts at mid-latitudes. *Contrib. Atmos. Phys.*, *50*, 78-88.
- Hess, G.D. 1990. Numerical simulation of the August 1986 heavy rainfall event in the Sydney area. *J. geophys. Res.*, *95 D3*, 2073-82.
- Holland, G.J., Lynch, A.H. and Leslie, L.M. 1987. Australian east-coast cyclones. Part I: Synoptic overview and case study. *Mon. Weath. Rev.*, *115*, 3024-36.
- Kessler, E. 1969. On the distribution and continuity of water substance in atmospheric circulations. *Met. Monogr.*, *10*, 1-84.
- Kuo, H-L. 1965. On formation and intensification of tropical cyclones through latent heat release by cumulus convection. *J. Atmos. Sci.*, *22*, 40-63.
- Leslie, L.M., Mills, G.A., Logan, L.W., Gauntlett, D.J., Kelly, G.A., Manton, M.J., McGregor, J.L. and Sardie, J.M. 1985. A high resolution primitive equations NWP model for operations and research. *Aust. Met. Mag.*, *33*, 11-36.
- Leslie, L.M., Holland, G.J. and Lynch, A.H. 1987. Australian east-coast cyclones. Part II: Numerical modelling study. *Mon. Weath. Rev.*, *115*, 3037-53.
- Louis, J.F. (ed.) 1984. ECMWF forecast model — physical parameterization. *Res. Man.* *3*, European Centre for Medium Range Weather Forecasts, Shinfield Park, Reading, Berks., England.
- McInnes, K.L. and Hess, G.D. 1992. Modifications to the Australian region limited area model and their impact on an east coast low event. *Aust. Met. Mag.*, *40*, 21-31.
- Monteith, J.L. 1964. Evaporation and environment. *Symp. Soc. Exp. Bio.*, *19*, 205-34.
- Paltridge, G.W. and Platt, C.M.R. 1976. *Radiative processes in meteorology and climatology*. Elsevier, 318 pp.
- Roach, W.T. and Slingo, A. 1979. A high resolution infrared radiative transfer scheme to study the interaction of radiation with cloud. *Q. Jl R. met. Soc.*, *105*, 603-14.
- Somieski, F. 1988. Mesoscale model parametrizations for radiation and turbulent fluxes at the lower boundary. *Oberpfaf-jenhofen: DFVLR-FB-88-48*.
- Staniforth, A. and Côté, J. 1991. Semi-Lagrangian integration schemes for atmospheric models — a review. *Mon. Weath. Rev.*, *119*, 2206-23.
- Wu, J. 1982. Wind stress coefficients over sea surface from breeze to hurricane. *J. geophys. Res.*, *87*, 9704-706.